




# Polycaprolactone-gelatin nanofibers incorporated with dual antibiotic-loaded carboxyl-modified silica nanoparticles

Zahra Gounani<sup>1,2,3,4</sup>, Sajedeh Pourianejad<sup>2,6</sup>, Mohammad Ali Asadollahi<sup>2,\*</sup> , Rikke L. Meyer<sup>4,5</sup>, Jessica M. Rosenholm<sup>3</sup>, and Ayyoob Arpanaei<sup>1,\*</sup>

<sup>1</sup>Department of Industrial and Environmental Biotechnology, National Institute of Genetic Engineering and Biotechnology, Tehran, P. O. BOX 1417863171, Iran

<sup>2</sup>Department of Biotechnology, Faculty of Biological Science and Technology, University of Isfahan, Isfahan 8174673441, Iran

<sup>3</sup>Pharmaceutical Sciences Laboratory, Faculty of Science and Engineering, Åbo Akademi University, 20520 Turku, Finland

<sup>4</sup>Interdisciplinary Nanoscience Center (iNANO), Aarhus University, 8000 Aarhus, Denmark

<sup>5</sup>Department of Bioscience, Aarhus University, 8000 Aarhus, Denmark

<sup>6</sup>Joint School of Nanoscience and Nanoengineering, University of North Carolina in Greensboro, Greensboro, USA

Received: 7 April 2020

Accepted: 1 September 2020

Published online:

21 September 2020

© Springer Science+Business Media, LLC, part of Springer Nature 2020

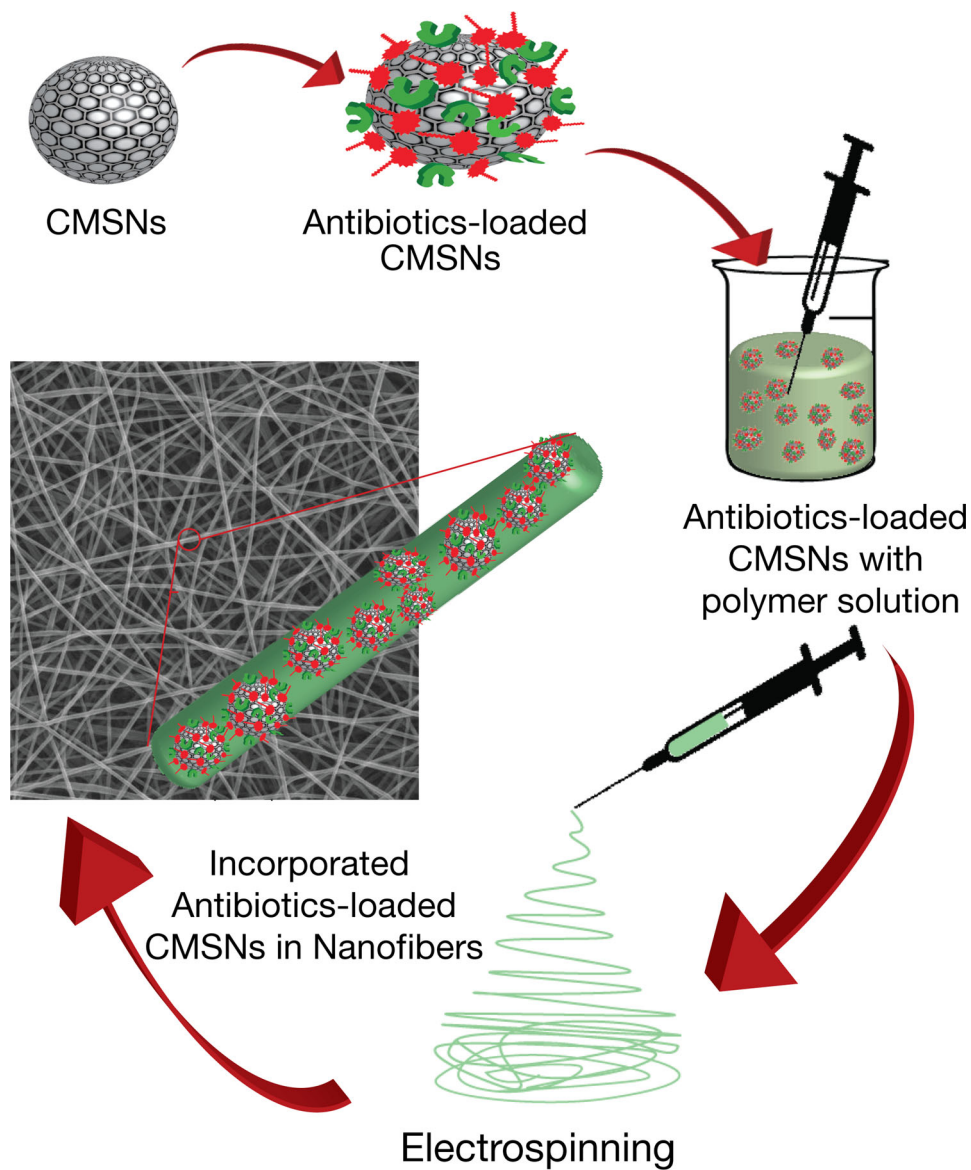
## ABSTRACT

In this study, we used electrospun polycaprolactone (PCL) or a mixture of PCL and gelatin (Gel) in a mixed acidic solvent to develop antimicrobial electrospun nanofibers. Carboxyl-modified mesoporous silica nanoparticles (CMSNs) or CMSNs loaded with antibiotic drugs polymyxin B and vancomycin (CMSNs/ABs) were mixed with the electrospinning solution in concentrations of 1%, 2.5% and 5%. The nanofibers diameter measured between 122 and 138 nm. Higher concentrations of gelatin or CMSNs increased hydrophilicity and degradability of the nanofibers. CMSNs enhanced nanofibers mechanical strength. PCL/Gel nanofibers incorporated with CMSNs/ABs (2.5% and 5%) showed high antibacterial efficiency against *Pseudomonas aeruginosa* and *Staphylococcus aureus*. Also bacterial cell adhesion decreased when 2.5% and 5% of CMSNs/ABs were incorporated in PCL/Gel mats. MTT and hemolysis assays indicated excellent biocompatibility of all types of electrospun nanofibers. This study confirms that a proper mixture of PCL, gelatin and CMSNs loaded with two antibiotics could offer antimicrobial activities with high biocompatibility and biodegradability properties.

Handling Editor: Annela M. Seddon.

Address correspondence to E-mail: ma.asadollahi@ast.ui.ac.ir; aa@nigeb.ac.ir

## GRAPHIC ABSTRACT



## Introduction

Bacterial infections involving biofilms are one of the most challenging issues for both acute and chronic wounds [1]. Wound infections are mostly polymicrobial infections involving numerous bacterial strains such as *Escherichia coli*, *Acinetobacter*

*calcoaceticus*, *Klebsiella pneumonia*, *Acinetobacter baumannii*, *Enterobacter cloacae* and the most common species *Pseudomonas aeruginosa* and *Staphylococcus aureus* [2]. Some commonly used antibiotics for wound infections include penicillin G, gentamicin, bacitracin, metronidazole, polymyxin B and vancomycin [3, 4]. Vancomycin is effective against Gram-

positive bacteria such as *S. aureus* and polymyxin B is effective against resistant Gram-negative bacteria, such as *K. pneumoniae*, *A. baumannii* and *P. aeruginosa* [5, 6]. The combination of two antibiotics has shown synergistic interaction against Gram-negative bacteria [7]. Polymyxin B targets the outer membrane of Gram-negative bacteria, forming electrostatic interaction between its positively charged diaminobutyric acid residue and negatively charged phosphate groups of membrane lipids. The lipopolysaccharide content of the cell wall is therefore destabilized, leading to permeability of outer membrane of bacteria and leakage of the cytoplasmic content and finally, cell death [8]. Vancomycin acts against Gram-positive bacteria by binding to peptidoglycan precursors and inhibiting cell wall cross-linking [9]. Vancomycin is not effective against Gram-negative bacteria, because their outer membranes are impermeable to large glycopeptide molecules. By combining polymyxin B and vancomycin, peptidoglycan layer of Gram-negative bacteria becomes accessible to vancomycin. Systemic administration of antibiotics like polymyxin B and vancomycin is associated with high risk of nephrotoxicity and neurotoxicity [10, 11]. However, wound infection management uses both systemic and topical administration. Local and topical administration of antibiotics has several advantages such as achieving high and sustained concentration of antibiotics at the site of infection, limited side effects, less antibiotics usage, and the possibility of applying antibiotics at home by patients [3].

Antimicrobial wound dressings play an important role in wound healing because they provide an essential hydrated and aerated environment and a barrier to external agents as well as preventing and eradicating infections. Electrospun nanofibrous mats offer excellent properties as wound dressings due to their porous texture, which provides aeration, drainage of wound exudates, high surface area, and similar morphology to extracellular matrix promoting skin cell growth and proliferation [12, 13]. Numerous studies on electrospun antimicrobial wound dressings have been reported during the past decades [14–16]. Many of these studies reported on the incorporation of antibiotics such as gentamycin and tetracycline in nanofibrous mats [17, 18]. However, the combination of antibiotics has been less considered in such studies. Moreover, there are few studies of encapsulation of toxic antibiotics in

nanofibers [19]. While in the case of highly toxic antibiotics with potential life-threatening side effects, topical administration becomes a priority. In this study, we developed an antibacterial electrospun nanocomposite of PCL and gelatin incorporated with combined antibiotics of vancomycin and polymyxin B (ABs). Polycaprolactone (PCL), as approved by the U.S. Food and Drug Administration (FDA) for use in drug delivery, is a polymer with high biocompatibility. It has suitable tensile properties for biomedical applications and has been one of the first candidate polymers for tissue engineering in the last decade [20]. However, PCL suffers from some disadvantages such as high hydrophobicity and slow biodegradability [21]. Gelatin is a biopolymer derived from collagen which has excellent cell recognition properties [22] but low mechanical strength and high solubility in physiological solutions [23, 24]. Therefore, mixing PCL and gelatin has been suggested as a successful strategy to overcome the drawbacks of both polymers while obtaining the sum of their advantages at the same time [20, 24, 25].

Mixing of PCL and gelatin has previously been carried out in a number of different solvents, such as trifluoroethanol (TFE) [20, 24], tetrahydrofuran (THF) [26, 27], hexafluoro-2-propanol [28], mixed organic solvent systems include dichloromethane [22, 29], methanol, chloroform, dimethyl formaldehyde [30] and acidic solvents like acetic acid [23, 31] and formic acid [17, 27]. We examined several solvent systems including a mixture of dichloromethane, DMF, methanol, water, acetic acid and formic acid at different ratios. The best results in terms of nanofiber diameter, reproducibility, and required time for dissolution of both polymers were obtained by an acidic solvent system of mixed (50:50) acetic acid and formic acid.

To incorporate both antibiotics into mixed polymer system, solubility of antibiotics into same solvent system is necessary. Hydrophilic antibiotics such as polymyxin B and vancomycin have poor solubility in organic and pure acidic solvents [32, 33]. To achieve homogenous dispersion of antibiotics in polymer solvents, we used carboxyl-modified mesoporous silica nanoparticles (CMSNs) as carriers for the antibiotics, as we found improved antibacterial activity and cytotoxicity for dual antibiotics-loaded into CMSNs compared to bare MSNs and amine-modified MSNs in our previous study [34]. Using mesoporous silica nanoparticles (MSNs) as carrier for antibiotics have

additional advantages, including improved mechanical properties and hydrophilicity of nanofibers [35, 36]. We hypothesized that incorporation of CMSNs would improve mechanical properties, degradability and hydrophilicity of the electrospun mat, while mixing PCL with gelatin would enhance degradability and hydrophilicity. We, therefore, evaluated the effect of nanoparticle concentration and PCL/Gel ratio on the nanofibers' structure, hydrophobicity, mechanical properties, degradability, and antimicrobial properties. Our study offers a formulation method for local and prolonged release of highly toxic antibiotics which are commonly used to combat multidrug resistance bacteria in chronic wounds.

## Materials and methods

### Materials

Polycaprolactone (PCL, Mw, 80000), gelatin from bovine skin Type B, Acetonitrile (99.98%), succinic anhydride, polymyxin B sulfate salt (polymyxin B) and vancomycin were purchased from Sigma-Aldrich (St. Louis, MO). Hexadecyltrimethylammonium bromide (CTAB), Tetraethyl ortosilicate (TEOS, 99%), NaOH, N-(2-aminoethyl)-3-aminopropyltrimethoxy-silane (AAPTMS), N,N-dimethylformamide (DMF), Trifluoroacetic acid (TFA, 99%), absolute ethanol (99.99%) and acetic acid glacial (99.98%), were purchased from Merck (Darmstadt, Germany). Formic acid 98.0% was obtained from Samchun Chemicals (South Korea). All materials and reagents related to antibacterial and cytotoxicity assays were purchased from Sigma-Aldrich (St. Louis, MO).

### Synthesis of electrospun mats

To dissolve PCL with gelatin, we tried different solvents; and finally, a mixture of 1:1 (v/v) formic acid and acetic acid was used to prepare 13% (w/v) polymer solution of PCL or PCL/Gel with proportion of 50:50 or 70:30 PCL/Gel (w/w). The PCL pellets and gelatin powder were dissolved completely in formic acid and acetic acid by stirring for up to 3 h. CMSNs loaded or unloaded with antibiotics (1.3, 3.15 and 6.5 mg) were added to 1 ml solution to make nanofibers with 1%, 2.5% and 5% of CMSN or

CMSNs loaded with combined vancomycin and polymyxin B (CMSN/ABs), respectively. The amounts of antibiotics in 1%, 2.5% and 5% of CMSN/ABs were calculated to be 0.39, 0.19, and 0.47 mg for polymyxin B and 0.95, 0.95, 1.95 mg for vancomycin, respectively [34]. The CMSN/ABs and CMSN were dispersed in polymer solution by 15-min sonication before electrospinning. Preparation of nanoparticles loaded with combined antibiotics has been described previously [34]. Briefly, nanoparticles were loaded with antibiotics by mixing 1 mg ml<sup>-1</sup> of CMSNs and 600 µg ml<sup>-1</sup> polymyxin B and 600 µg ml<sup>-1</sup> vancomycin in HEPES buffer. The mixture was rotary stirred at 4 °C overnight, and the day after the nanoparticles were centrifuged and washed twice in HEPES buffer. The amount of loaded antibiotics was calculated from drug concentrations in all supernatants. CMSNs were loaded with a ratio of 300:150 µg/mg of polymyxin B to vancomycin which showed a superior antibacterial activity comparing to other ratios in our previous study [34]. An electrospinning setup with a plastic syringe fitted with a stainless-steel needle (gauge 23) and a syringe pump (JMS, Model SP-500) operated at 0.3 ml/h was used to prepare the PCL and PCL/Gel nanofibers. A high-voltage-power supply (EMERSUN, TDGC<sub>2</sub>) connected to the needle tip provided an output voltage of 18 kV to deposit PCL and PCL/Gel nanofibers on a grounded aluminum foil collector placed 15 cm from the tip.

### Characterization of nanofibers

The size, morphology and structure of nanoparticles were reported in our previous work [37]. The morphology and size of the nanofibers were observed using scanning electron microscopy (SEM, JEOL JSM-5600LV, Japan) with an accelerating voltage of 15 kV. In preparation for SEM, samples were sputter coated with gold films with a thickness of 10 nm. The size distribution of the electrospun fibers was analyzed using ImageJ 1.47G software. At least 200 nanofibers at different images were analyzed for each sample. The distribution of nanoparticles inside the nanofibers was analyzed by transmission electron microscopy (at least 20 images per sample) (TEM, Zeiss EM10C). The chemical composition of the nanofibers was analyzed by collecting attenuated total reflection Fourier transform infrared (ATR-FTIR) (JASCO FT/IR 6300 spectrometer, Easton, MD) spectra, in the

wave number range of 4000–600  $\text{cm}^{-1}$  at room temperature. The mechanical properties of the electrospun fibrous mats were examined using a material testing machine (H5K-S, Hounsfield, UK) with an elongation speed of 10 mm/min at room temperature. Three strips from different sites of each nanofiber sample were chosen for the tensile test, and specimens were cut into rectangular pieces (5 mm  $\times$  30 mm). The tensile testing was performed with a loaded cell of 10 N under room temperature. Hydrophilicity of the mats was determined by measuring contact angle of the electrospun mats by a video contact angle system (VCA Optima, AST Products Inc, Billerica, MA). Five samples were used for each test and results were expressed as mean  $\pm$  standard deviation (SD).

### In vitro degradation of mats

In vitro degradation of mats (1  $\times$  1 cm,  $n = 3$ ) was studied in phosphate-buffered saline (PBS) (2 ml) at pH 7.4, 37 °C during 1, 2, 4, 7 and 14 days. After removing the buffer solution, samples were washed with deionized water, dried in oven at 60 °C for 48 h. Mass loss (%) was defined as  $(W_0 - W_t)/(W_0) \times 100$ , where  $W_0$  is the initial mass of the dry mats and  $W_t$  is the mass of mats at time  $t$ .

### Release profile of antibiotics from electrospun mats

Samples (diameter 1 cm, thickness 0.2 mm,  $n = 3$ ) were incubated in 1.5 ml PBS at 37 °C for time intervals of 2, 4, 6, 12, 24, 48, 96 and 148 h. At each time point, PBS was collected and centrifuged (19000 $\times$ g, 20 min) to precipitate nanoparticles before analysis by HPLC. HPLC analysis was carried out by a Merck- Hitachi 7000 HPLC on a Gemini<sup>®</sup> C18 110 Å, 3  $\mu\text{m}$  particle size, 4.6  $\times$  150 mm column. The mobile phase was a gradient of buffer A [0.1% trifluoroacetic acid (TFA) in MQ] to buffer B (0.1% TFA). The flow rate was set to 1 ml  $\text{min}^{-1}$ , and the injection volume was 10  $\mu\text{l}$ . The gradient was programmed as 5–65% of B for 20 min, 65–100% of B for 1 min, constant at 100% B for 4 min, 100% B to 5% B in 2 min, constant at 5% B for 2 min., and the absorbance was monitored at 220 nm for polymyxin B and 280 nm for vancomycin. Standard solutions of 10/5–40/20  $\mu\text{g}/\text{ml}$  of polymyxin B/vancomycin dissolved in PBS were used for calibration.

Calibration curves obtained were linear with  $R^2$  values of 0.99.

### Antibacterial activity of mats

The antimicrobial activity of mats was studied against two common wound pathogens, the Gram-negative *P. aeruginosa* PAO1 (DSM 19880) and Gram-positive *S. aureus* (DSM20231). UV-sterilized mats (laminar hood UV germicidal lamps, 245 nm, 20 min for each side) (diameter 1 cm, thickness 0.2 mm,  $n = 3$ ) was incubated in 48 well plates containing 800  $\mu\text{l}$  of  $10^6$  CFU/ml bacterial solution made by dilution an overnight culture and incubated at 37 °C for 24 h. The day after, antibacterial efficiency of mats was estimated by measuring optical density at 600 nm ( $\text{OD}_{600}$ ) using UV–visible spectrophotometer and antibacterial efficiency (%) was determined by  $(1 - A_{\text{sample}}/A_{\text{positive control}}) * 100$ . Antibacterial activity of mats was further surveyed by agar diffusion method for those fibers with considerable antibacterial effects from previous section. For that purpose, 100  $\mu\text{l}$  of overnight culture of *S. aureus* or *P. aeruginosa* suspension diluted in growth media to  $\text{OD}_{600} = 0.1$  was spread on Mueller-Hinton agar (MHA) plates. Then, mats disks (diameter 1 cm, thickness 0.2 mm,  $n = 3$ ) were gently placed on agar plates and inhibition zones were measured (mm) after overnight incubation at 37 °C (3 replications were used for different nanofibers). Mats containing nanoparticles without antibiotics were used as positive control. The antibacterial activity of nanofibers was also surveyed by time-kill assay. Based on the above analysis results, time-kill assay was carried out only for mats showing more than 10% antibacterial efficiency. Mats (diameter 1 cm, thickness 0.2 mm,  $n = 3$ ) were incubated in 48 well plates containing 1 ml of  $10^6$  CFU/ml bacterial solution in MHB media at 37 °C for 24 h. Aliquots (100  $\mu\text{l}$ ) were withdrawn at 2, 4, 6, 12, 24 h and after spreading on MH agar were incubated overnight at 37 °C before enumeration of CFU. To visualize antibacterial efficiency of mats, nanofibrous mats were analyzed by SEM, after incubating with  $10^6$  CFU/ml of *P. aeruginosa* solution in MHB at 37 °C for 24 h. After incubation, all nanofibers were gently washed with PBS five times and once with deionized water and were left to dry in room temperature. Samples were sputter coated with carbon after mounting on sample holders. SEM was carried out by a LEO Gemini 1530<sup>®</sup> (Zeiss, Oberkochen, Germany)

with a Thermo Scientific UltraDry Silicon Drift Detector (SDD).

### Biofilm inhibition assay

An MTT colorimetric method based on the reduction of a tetrazolium salt was used to determine cell viability of biofilm inhabitants. Single colonies of each bacteria were used for inoculation of 10 ml MHB media and incubated at 37 °C for 20 h to develop an overnight culture. The prepared overnight cultures were then diluted to bacterial concentration of  $5 \times 10^7$  CFU/ml and added to 48 well polystyrene plates (800  $\mu$ l per well) and incubated at 37 °C for 30 min. Then, the bacterial suspensions were replaced with fresh MHB media and nanofibrous mats (diameter 1 cm, thickness 0.2 mm,  $n = 3$ ) were added to each well and incubated for 24 h at 37 °C. Nanofibers without antibiotics and water were used as positive and negative control, respectively. At the end of the incubation, the culture media were gently removed by aspiration and replaced with 200  $\mu$ l of 10  $\mu$ M MTT in PBS and incubated for 4 h at 37 °C. The MTT solution was then removed and replaced with 200  $\mu$ l dimethyl sulfoxide (DMSO) and incubated for 1 h to solubilize the formazan crystals formed in the wells. The solution of each well was transferred to cuvettes and the absorbance of the solutions was measured at 540 nm using a UV–visible spectrophotometry. The biofilm formation percentage was calculated as “(sample absorbance-negative control absorbance)/(positive control absorbance-negative control absorbance)  $\times$  100.”

### Confocal laser scanning microscopy

For microscopy assay, biofilm formation was carried out in a 48-well polystyrene plate as it was described in previous section. Briefly, 48-well polystyrene plates were inoculated with a bacterial solution (800  $\mu$ l per well) containing  $5 \times 10^7$  CFU/ml and then incubated for 30 min at 37 °C, followed by replacement of the bacterial suspension with fresh MHB media containing nanofibrous mats (diameter 1 cm, thickness 0.2 mm,  $n = 3$ ) loaded with antibiotics. For negative control wells, same amount of fresh media was added but mats were not loaded with antibiotics. The plate was then incubated for another 24 h at 37 °C before removing the media, rinsing five times with 200  $\mu$ l sterile PBS, and adding

200  $\mu$ l PBS containing 2  $\mu$ M of the membrane-permeant DNA-binding stain, SYTO 9 (Thermo Fisher Scientific), and 10  $\mu$ M of the membrane-impermeant nucleic acid-binding stain, propidium iodide (Thermo Fisher Scientific) for visualization of dead cells. The plates were incubated at room temperature for 20–30 min with the staining solution. The nanofibrous mats were then removed from the plate and placed on glass slides and covered by cover slips. Slides were imaged by a Zeiss LSM780 (Jena, Germany) using a Plan-Apochromat 100x/1.40 Oil immersion objective, and excitation with 488 nm and 543 nm lasers.

### Cytotoxicity of nanofiber mats

*MTT assay:* The cytotoxicity of the mats was investigated against mouse fibroblast cell line, L929, by MTT assay (3 replications). The nanofiber mats (diameter 1 cm, thickness 0.2 mm,  $n = 3$ ) were sterilized with UV radiation for 20 min on each side. The mats were then placed in a 48-well plate and plated by  $10^4$  cells per well in Dulbecco’s modified Eagle’s medium (DMEM) with 10% fetal bovine serum, and incubated at 37 °C, 5% CO<sub>2</sub> for 3 and 7 days. After treatment, the media were removed. The cells were washed with PBS and incubated with 100  $\mu$ l of MTT-containing medium (0.5 mg/ml) for 4 h. The medium was then removed and 100  $\mu$ l DMSO was added to wells and incubated for another 1 h in dark. The absorbance of the solution was read at 570 nm by using a microplate ELISA reader (Bio-Rad, USA). Growth media with no nanofiber were used as negative control. The cell viability was calculated as “(sample absorbance)/(negative control absorbance)  $\times$  100.”

*Hemolysis assay:* To study hemolytic effects of mats, (EDTA)-stabilized human red blood samples (donated by a healthy volunteer and collected by a licensed practical nurse) and were centrifuged (2000 $\times$ g for 10 min) to remove plasma, buffy coat, and top layer of cells. The remained red blood cells (RBCs) were washed five times with sterile PBS. After washing, packed RBCs were diluted 20 times in PBS. Diluted RBCs (200  $\mu$ l) were added to 800  $\mu$ l PBS containing different mats (diameter 1 cm, thickness 0.2 mm,  $n = 3$ ) PBS and water (800  $\mu$ l) with no mat were used as negative and positive control, respectively. Samples were then incubated at room temperature for 2 h, followed by centrifugation (2000 $\times$ g, 10 min) and the absorbance of the supernatants was

recorded with microplate ELISA reader (Bio-Rad, USA) at 541 nm. The hemolytic percentage was calculated as “(sample absorbance –negative control absorbance)/(positive control absorbance–negative control absorbance) × 100.”

### Statistical analysis

Two-way ANOVA tests (SPSS) was performed to calculate differences for experiments with multiple data sets. A Tukey’s multiple comparison procedure was performed between groups with significant differences.

## Results and discussion

### Characterization of nanofibers

The thickness of synthesised mats was about  $165 \pm 10 \mu\text{m}$ . Size distribution and morphology of nanofibers were studied by SEM. The electrospun fibers were uniform in diameter size (Fig. 1). SEM images showed slightly (not significantly) larger diameter and less homogenous diameter distribution of nanofibers at increasing concentrations of gelatin or CMSNs (Table S1), which could be attributed to the enhanced viscosity of nanofibers when adding gelatin or CMSNs [38]. The results are consistent with previous studies reporting larger diameters of nanofibers by increasing the amount of embedded nanoparticles [35, 39]. The diameter of nanofibers varied in a small range (156–179 nm) across all different synthesis conditions. Incorporation of nanoparticles inside nanofibers was confirmed by TEM micrographs (Fig. 2).

Hydrophilicity of nanofibers was evaluated by measuring the incident contact angle. Reduced contact angle was observed for PCL/Gel mats in compare to PCL mats. Also, hydrophilicity of mats was enhanced with increasing CMSNs concentration in agreement with previous reports [35, 40] (Table S1). The nanofibrous mats containing 50% gelatin and 5% CMSNs showed the lowest contact angle implying highest hydrophilicity. The higher hydrophilicity of nanofibers with gelatin and CMSNs could be due to presence of ionic groups such as carboxyl groups on the surface of CMSNs and carboxyl and amine functional groups in gelatin [35]. These results were not correlated to improved mechanical properties, as

lowest Young’s moduli were found for nanofibers containing 50% gelatin. However, increasing the concentration of CMSNs enhanced Young’s moduli of all three groups of nanofibrous mats including PCL, PCL/Gel30 and PCL/Gel50.

ATR-FTIR analysis was carried out for surface chemistry characterization of nanofibers. Figure S1 shows the FTIR spectra of pristine antibiotics, PCL, PCL/2.5%CMSNs, PCL/2.5%CMSNs/ABs, PCL/Gel30, PCL/Gel30/2.5%CMSNs and PCL/Gel30/2.5%CMSNs/ABs. Infrared spectra for PCL-related stretching modes were observed for all samples. These include  $2949 \text{ cm}^{-1}$  (asymmetric CH<sub>2</sub> stretching),  $2860 \text{ cm}^{-1}$  (symmetric CH<sub>2</sub> stretching),  $1727 \text{ cm}^{-1}$  (carbonyl stretching),  $1295 \text{ cm}^{-1}$  (C–O and C–C stretching) and  $1240 \text{ cm}^{-1}$  (asymmetric COC stretching). Bands of protein related to gelatin appeared at  $1645 \text{ cm}^{-1}$  (amide I) and  $1540 \text{ cm}^{-1}$  (amide II),  $3200 \text{ cm}^{-1}$  (alcohol C = O stretching) and around  $3050 \text{ cm}^{-1}$  (carboxylic acid C = O stretching) [17]. Typical peak of Si–O–Si was observed at  $1090 \text{ cm}^{-1}$  [40]. Presence of vancomycin and polymyxin B was confirmed in the region below  $1800 \text{ cm}^{-1}$  and at  $3270 \text{ cm}^{-1}$  (C = O stretching) [19].

### In vitro degradation of mats

The in vitro degradation of all nanofibers, estimated by weight loss measurements, is shown in Fig. 3. Pure PCL weight loss was 1.2% after 2 weeks which increased to 21.44% and 51.96% for PCL/Gel30 and PCL/Gel50, respectively. Since gelatin is easily dissolved at temperatures around  $40 \text{ }^\circ\text{C}$ , it is not surprising that increasing gelatin concentration improves degradability of PCL. The addition of CMSNs to PCL, PCL/Gel30 and PCL/Gel50 increased degradation percentage, as was expected. CMSNs with high surface area containing hydrophilic carboxyl groups can adsorb water molecules which subsequently causes swelling of nanofibers, thereby increasing their degradation [41]. The highest degradability was obtained for PCL/Gel50/5%CMSNs so that samples were mostly dissolved after two weeks incubation in PBS at  $37 \text{ }^\circ\text{C}$ .

### Release profiles of two antibiotics from nanofibers

The release profile of antibiotics has a significant influence on their antibacterial effects [13]. We

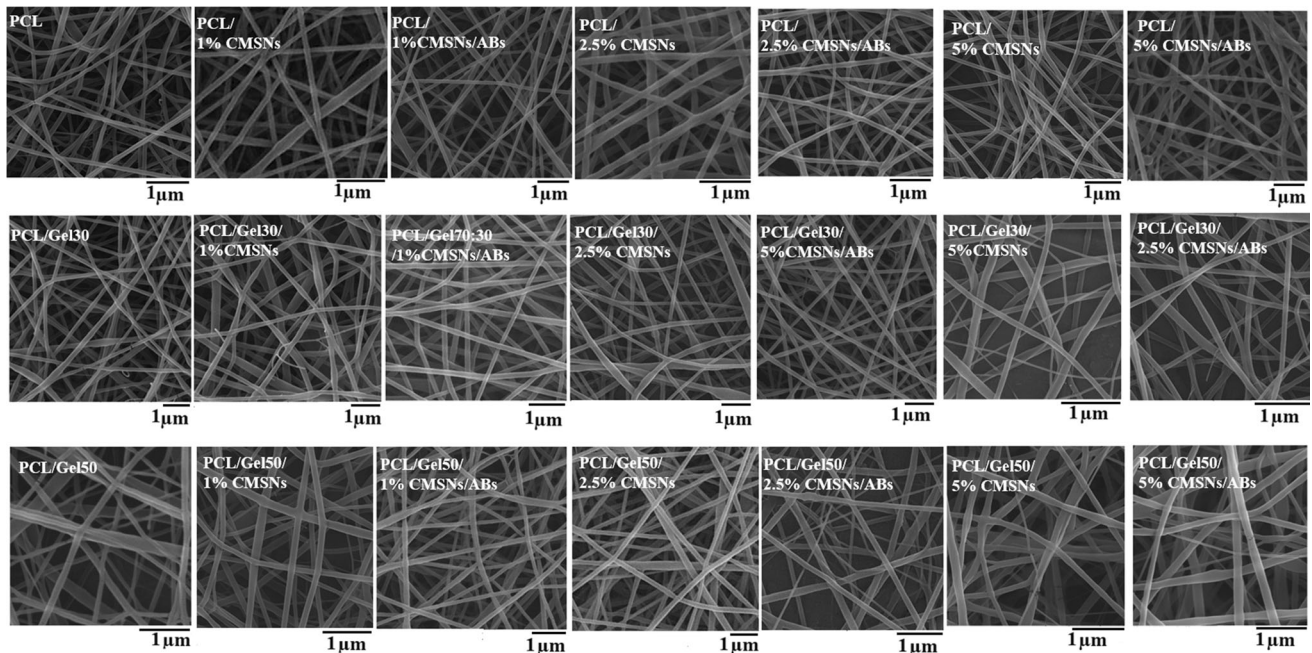


**Figure 1** SEM micrographs of nanofibers morphology. Different nanofibers were synthesized from PCL or PCL/Gelatin with two ratio of 70:30 (PCL/Gel30) and 50:50 (PCL/Gel50). All three type

of nanofibers were also mixed with 1% CMSNs, 2.5% CMSNs and 5% CMSNs or antibiotics loaded CMSNs (CMSNs/ABs) with the same ratios.

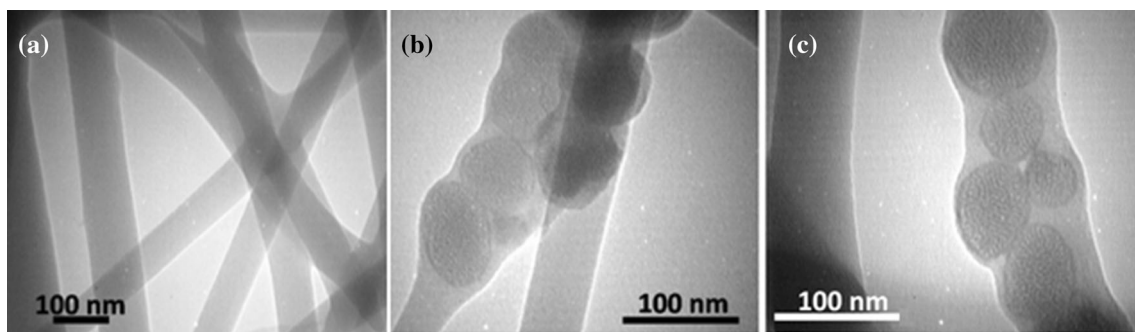


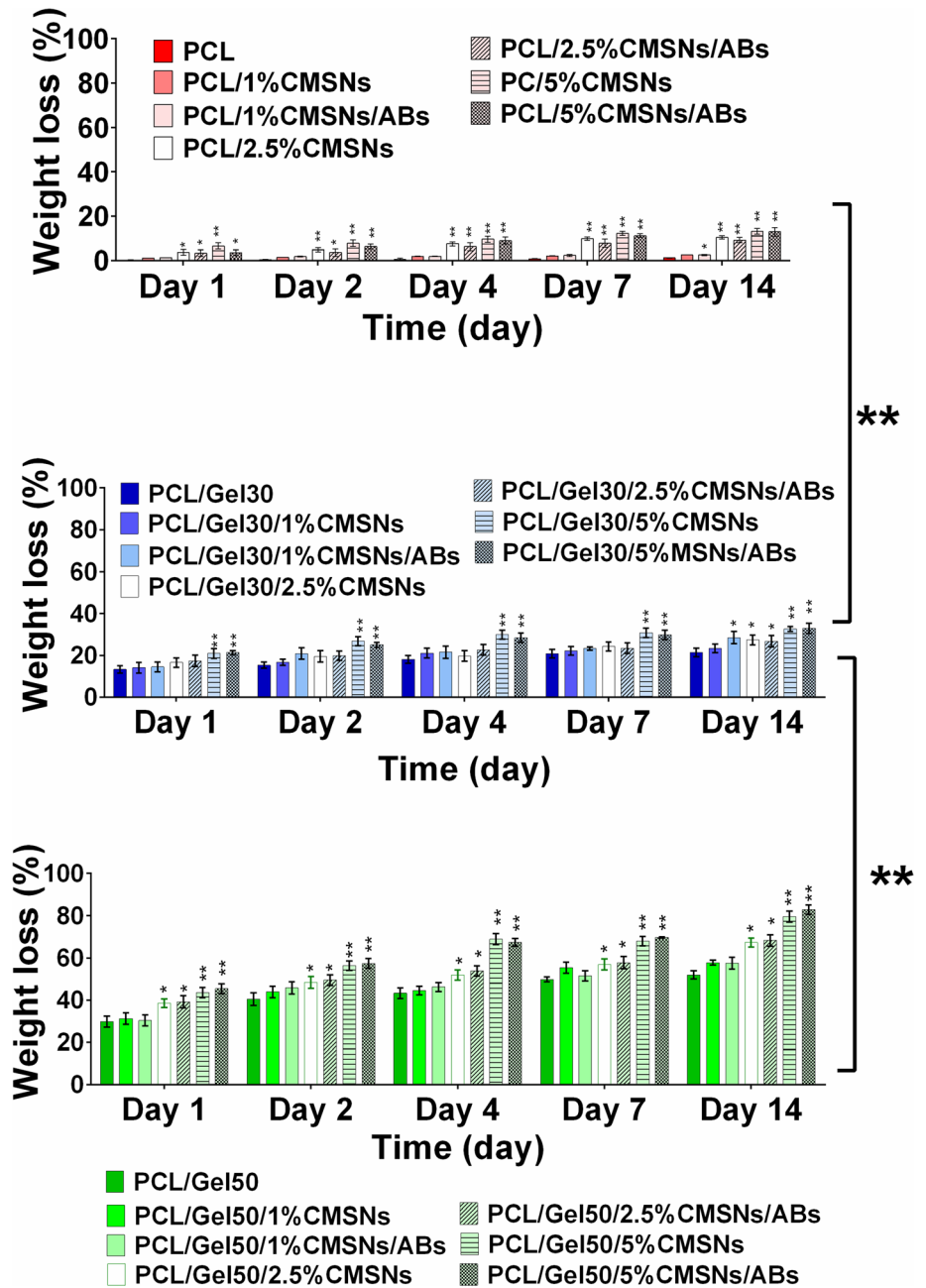
**Figure 2** TEM images of PCL/Gel30 nanofibers without CMSNs (a) and with CMSNs (5%) (b and c).

studied the release profiles only for samples with antibiotics-loaded CMSNs. Chromatographs of standard solutions and calibration curves for both antibiotics are presented in Fig. S2. PCL/2.5% CMSNs/ABs and PCL/5% CMSNs/ABs showed a low degree of release, which was expected due to their low degradability (Fig. 4). The release from 1% nanofiber mats was lower than detection limit by HPLC, however, from antibacterial experiments, it can be estimated that the amount released did not exceed the minimum inhibitory concentration (MIC) of polymyxin B and vancomycin for *P. aeruginosa* and *S. aureus*. MIC of vancomycin against *S. aureus* and polymyxin B against *P. aeruginosa* were obtained

$0.5 \mu\text{g ml}^{-1}$  and  $1\text{--}2 \mu\text{g ml}^{-1}$ , respectively [37]. The addition of gelatin increased the antibiotics release rate, which could be due to the higher solubility and degradability of gelatin in buffer medium [42]. Release from PCL nanofibers is mostly governed by diffusion, while release from PCL/Gel nanofibers is governed by both degradation and diffusion [42]. Higher release from mats containing 5% CMSNs compared to the ones with 2.5% CMSNs is mostly related to a higher amount of antibiotics in mats with 5% CMSNs. However, the increased release percentage of mats containing 5% CMSNs can also be a result of higher degradability of mats with higher amount of CMSNs. Our results, consistent with previous



**Figure 3** Weight loss percentage profiles of the different mats after incubation in PBS (10 mM, pH 7.4) in different time points. All values were expressed as mean  $\pm$  SD ( $n = 3$ ). \* ( $p < 0.01$ ) and \*\* ( $P < 0.0001$ ) on the columns shows significant degradation rate of nanofibers containing CMSNs compared to those without CMSNs measured in same day. Adding gelatin to PCL increased degradation rate significantly. Data were analyzed by two-way ANOVA and Tukey's multiple comparison tests.



studies, showed that when MSNs were blended with synthetic polymers such as PCL, the degradation rate of nanofibers was increased [43, 44]. The effect of CMSNs in increasing the drug release could be concluded from higher degradation rate of nanofibers containing CMSNs compared to those without CMSNs [40]. The release profile of antibiotics is an important factor to consider when developing antimicrobial wound dressings. Polymeric nanofibers mostly release drug up to 90% during the first hour, which is a major disadvantage in case wound

dressing or tissue engineering applications are intended [38, 45, 46]. In the present study, all tested nanofibrous mats provided sustained release of both antibiotics for a duration of 96 h. We were not able to compare release profiles of free antibiotics with those that were loaded onto MSNs, since antibiotics were not soluble in solvents of polymeric solution. However, several previous studies have reported more prolonged release profile after loading drugs onto MSNs [47, 48].

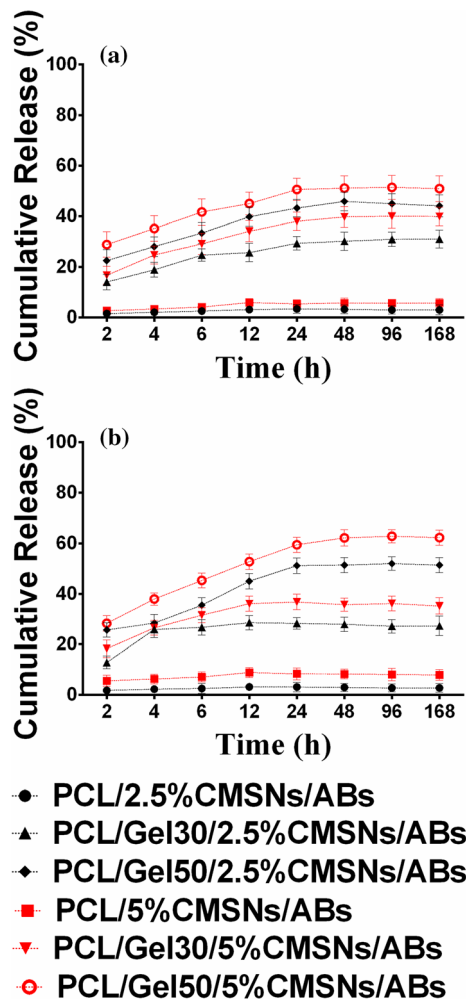


**Figure 4** Release profile of polymyxin B (a) and vancomycin (b) from mats at PBS (pH 7.4, 37 °C). All values were expressed as mean  $\pm$  SD (n = 3).

Sustained release of antibiotics from nanofibers could be explained by the fact that antibiotics need to be firstly released from nanoparticles to the matrix of nanofibers and then to the buffer solution, resulting in slower diffusion of antibiotics. Also, it is likely that there are electrostatic interactions between antibiotics and gelatin molecules that did not dissolve yet and remain inside the nanofiber texture, thereby preventing release of antibiotics from nanofibers. Gelatin type B, which was used in this project, has a negative charge at pH 7.4 opposite to both polymyxin B and vancomycin antibiotics which are positively charged at pH 7.4 [49]. Lower release rate of polymyxin B, which has higher positivity than vancomycin, supports this claim (Fig. 4).

### Antibacterial activity of nanofibers

The antibacterial efficiency of all mats was tested against *S. aureus* and *P. aeruginosa*. As expected, no antibacterial effect was observed for PCL, PCL/Gel30 and PCL/Gel50 and their corresponding mats incorporated with unloaded CMSNs (Fig. S3). Also, the nanofibers containing 1% antibiotics-loaded CMSNs did not show considerable bacteriostatic effects. The amount drug released from 1% nanofibrous mats was lower than detection limit by HPLC, however, from antibacterial experiments it can be estimated that released drugs did not exceed the minimum inhibitory concentration (MIC) of polymyxin B and vancomycin for *P. aeruginosa* and *S. aureus*. MIC of vancomycin against *S. aureus* and polymyxin B against *P. aeruginosa* were obtained  $0.5 \mu\text{g ml}^{-1}$  and  $1\text{--}2 \mu\text{g ml}^{-1}$ , respectively [37]. In contrast, PCL/Gel30 and PCL/Gel50 containing 2.5% and 5% antibiotics-loaded CMSNs exhibited remarkable bacteriostatic effects after 24 h. The antibacterial effects of mats containing 2.5% and 5% antibiotics-loaded CMSNs were further investigated by time-kill assays (Fig. 5). Results revealed that PCL/2.5%CMSNs/ABs and PCL/5%CMSNs/ABs inhibited bacterial growth, but they did not cause a significant decrease in the number of viable bacterial cells. Only nanofibers prepared with gelatin (PCL/Gel 30/2.5%/ABs and PCL/Gel50/2.5% CMSNs) killed significant number of *P. aeruginosa* and *S. aureus* during the 24 h incubation. PCL/Gel30/5%CMSNs/ABs showed bactericidal effect against both strains during 24 h, while PCL/Gel 50/5%CMSNs/ABs killed all cells of both strains during 12 h and 8 h, respectively.

To visualize morphological changes of mats after incubation with bacterial cells, nanofibers were analyzed by SEM after incubation with *P. aeruginosa* for 24 h. As seen in Fig. 6, PCL nanofibers containing 2.5 and 5% antibiotics-loaded CMSNs were completely covered by biofilm, while PCL/Gel30 and PCL/Gel50 containing same amounts of antibiotics-loaded CMSNs showed no evidence of bacterial growth. It can be noted from SEM images (Fig. 6) that PCL/Gel nanofibers containing 2.5% CMSNs showed no apparent morphology change after 24 h incubation with bacterial solution, while PCL/Gel mats containing 5% CMSNs started to degrade during same time of incubation, which is confirmation of our

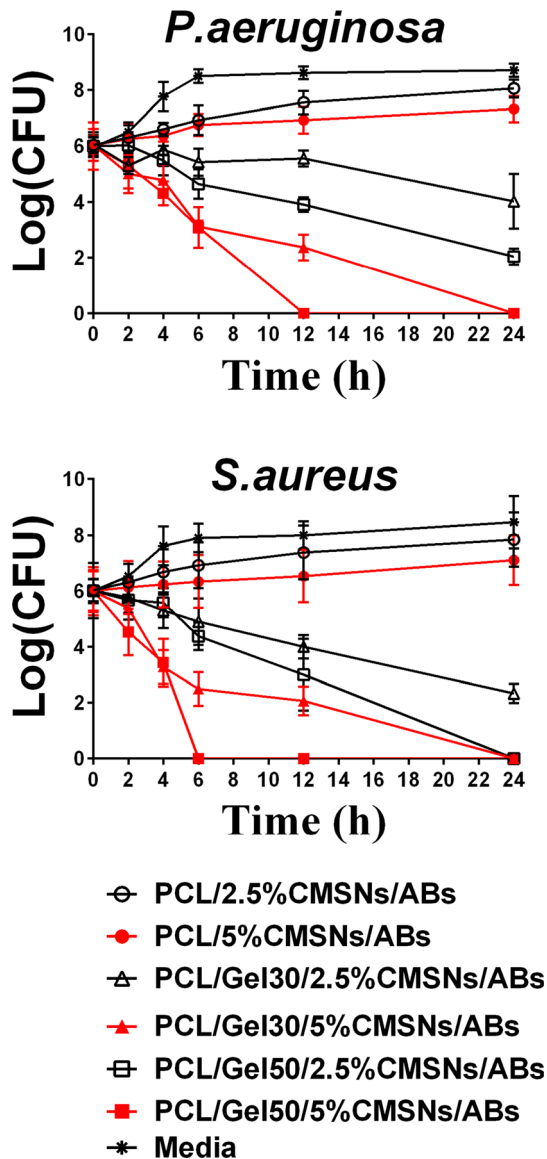


**Figure 5** Time-kill curves of mats against *P. aeruginosa* and *S. aureus*. CFU numeration was carried out during 24 h and in time points of 0, 2, 4, 6, 12 and 24 h. All values were expressed as mean  $\pm$  SD (n = 3).

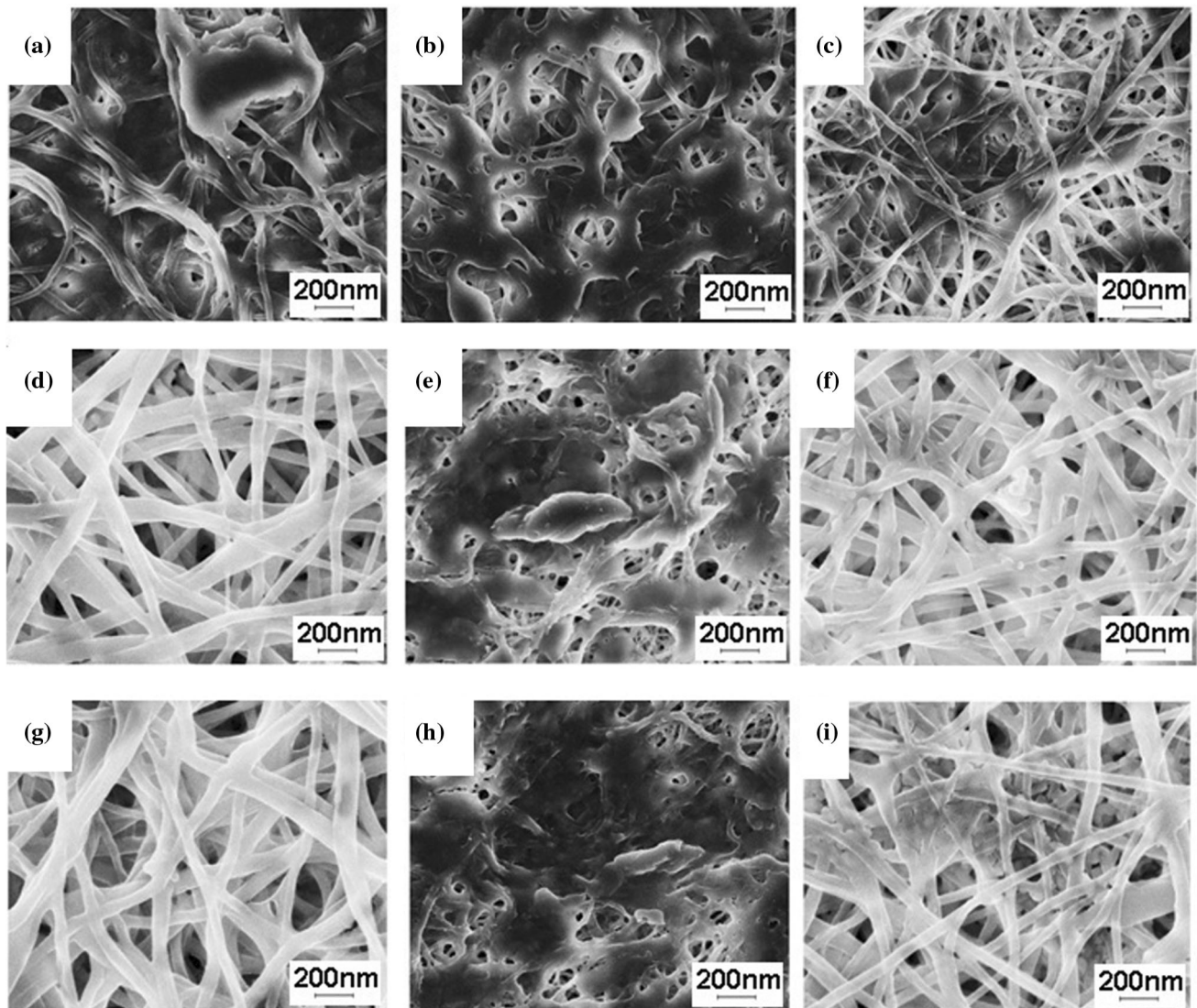
earlier claim that increasing CMSNs concentration leads to higher degradability of nanofibers.

Agar diffusion assays confirmed previous results (Fig. S4, Table S2). No inhibition zone was observed for PCL/2.5%CMSNs/ABs, and a smaller inhibition zone was observed for PCL/5%CMSNs/ABs in comparison to those of PCL/Gel30 and PCL/Gel50, indicating lower release rate of antibiotics from nanofibers that did not contain gelatin. Mats containing 5% CMSNs loaded with antibiotics revealed a bigger inhibition zone than those containing 2.5%

CMSNs. However, higher release rates were obtained for mats PCL/Gel50 than PCL/Gel30 containing same amount of antibiotics in release assay. In agar diffusion assay, PCL/Gel50 showed only a slightly bigger inhibition zone than PCL/Gel30. In a firm medium like agar, lower dissolution of gelatin occurs and thereby gelatin has smaller role in release rate than in a liquid buffer. All antibacterial assays indicated higher efficiency of mats against *S. aureus* compared to *P. aeruginosa*. It could be explained by higher release rate of vancomycin than polymyxin B from mats (Fig. 4b). On the other hand, MIC of vancomycin against *S. aureus* is lower than MIC of polymyxin B against *P. aeruginosa* [37], which can be another reason of slightly higher efficiency of mats against *S. aureus* than *P. aeruginosa*.

### Biofilm inhibition

Biofilm formation is a significant risk of both chronic and acute infections due to loss of innate barrier of skin [50]. The activity of nanofibrous mats in preventing biofilm formation was examined against *P. aeruginosa* and *S. aureus*. As expected, the nanofiber mats without antibiotics allowed biofilm formation of both species. In contrast, PCL/2.5%CMSNs/ABs and PCL/CMSNs5%/ABs decreased biofilm formation by 20% and 30% for *P. aeruginosa* and *S. aureus*, respectively, (Fig. S5). PCL/Gel30/2.5%CMSNs/ABs and PCL/Gel50/CMSNs-2.5%/ABs inhibited biofilm formation by 70%, while PCL/Gel30/5%CMSNs/ABs and PCL/Gel50/5%CMSNs/ABs prevented biofilm formation completely. The higher release percentage and higher antibiotics concentration in PCL/Gel30/5% CMSNs/ABs cause enhanced antibiofilm properties compared to other tested mats. The confocal images of the mats confirmed that PCL nanofibers even when they contain 2.5% and 5% antibiotics-loaded CMSNs were not very efficient against biofilm formation (Fig. 7). However, the addition of gelatin significantly increased the efficiency of mats against biofilm formation, which is clearly because of a higher release fraction of antibiotics from mats containing gelatin compared to PCL mats. Comparison of CLSM images of biofilm formation on PCL/Gel30 and PCL/Gel50 mats containing 2.5% or 5% antibiotics-loaded CMSNs reveals that increasing the concentration of CSMNs/ABs from 2.5 to 5% leads to decreased density of bacterial cells on the mats (Fig. 7). It could be due to higher



**Mag=30.00 KX EHT= 5.00 kV Aperture Size=10.00  $\mu$ m**  
**WD= 7mm Signal A=InLens Image Pixel Size=3.9 nm**

**Figure 6** SEM micrographs of nanofibrous mats after incubation with *P. aeruginosa* for 24 h. From upper left to bottom right: PCL/2.5%CMSNs/ABs (a), PCL/5%CMSNs (b), PCL/5%CMSNs/ABs (c), PCL/Gel30/2.5%CMSNs/ABs (d), PCL/Gel30/5% CMSNs (e), PCL/Gel30/5%CMSNs/ABs (f), PCL/Gel50/2.5% CMSNs (g), PCL/Gel50/5% CMSNs (h) and PCL/Gel50/5% CMSNs/ABs

(i). PCL/5%CMSNs (b), PCL/Gel30/5%CMSNs (e) and PCL/Gel50/5%CMSNs (h), the mats without antibiotics, clearly allowed bacterial growth. Degradation of PCL/Gel30/5%CMSNs/ABs and PCL/Gel50/5% CMSNs/ABs mats could be seen in the SEM micrographs (f) and (i), respectively.

and faster release of antibiotics from mats containing 5% CMSNs/ABs than those containing 2.5% CMSNs/ABs, as it was also shown in release assay.

Based on these findings, nanofibrous mats of PCL/Gel30 and PCL/Gel50 containing 5% CMSNs/ABs could completely inhibit biofilm formation (Fig. 7).

Compared to previous reports, the nanofibrous mats formulated in this study exhibited high anti-biofilm efficiency against two main bacterial strains responsible for chronic wound biofilms [51, 52]. Both acute and chronic wounds are subject to infection by *P. aeruginosa* and *S. aureus* [50]. The biofilm formation

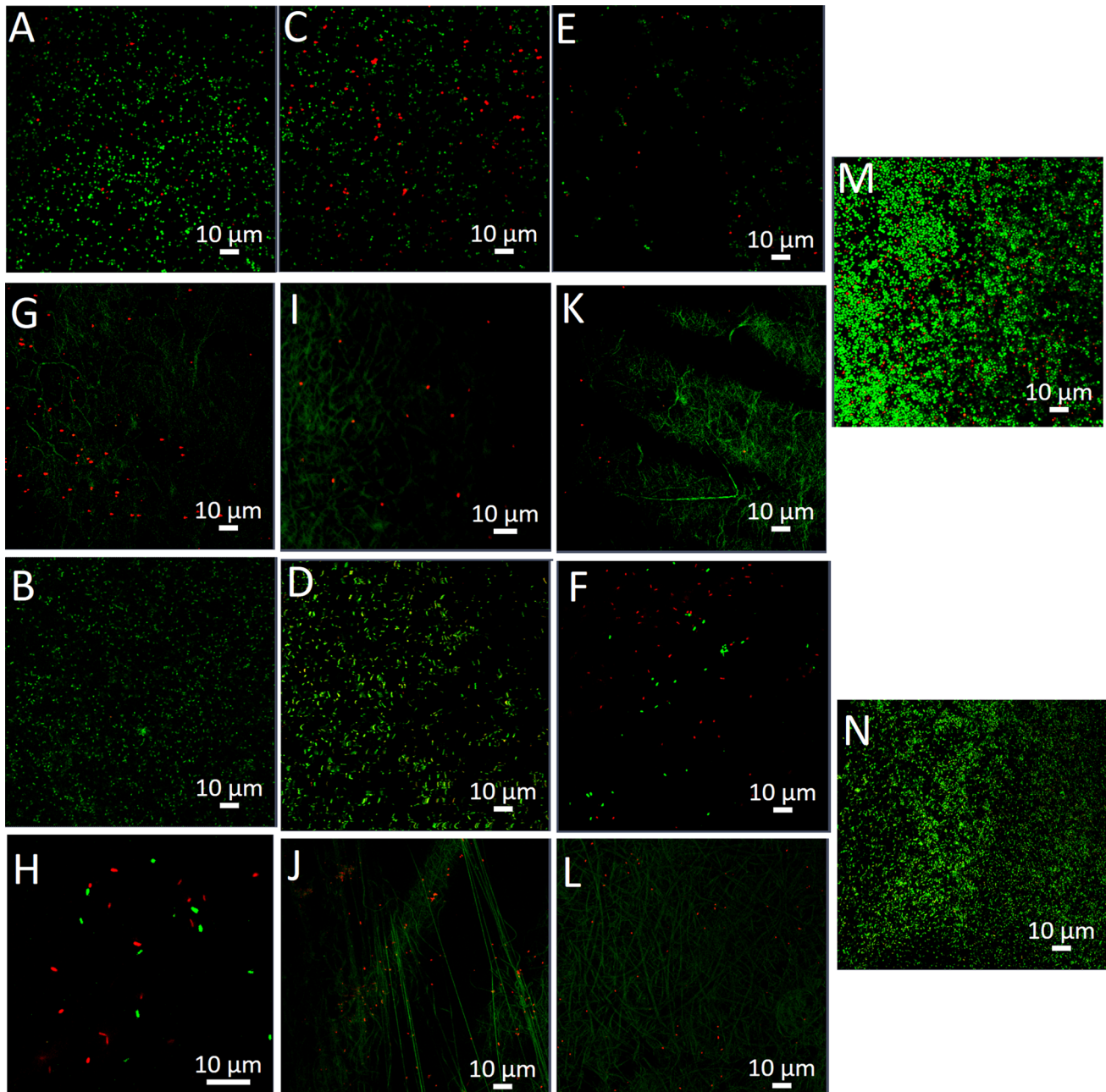


**Figure 7** Biofilm formation on PCL/CMSNs2.5%/ABs (A; *S. aureus*, B; *P. aeruginosa*), PCL/CMSNs5%/ABs (C; *S. aureus*, D; *P. aeruginosa*), PCL/Gel30/CMSNs2.5%/ABs (E; *S. aureus*, F; *P. aeruginosa*), PCL/Gel30/CMSNs5%/ABs (G; *S. aureus*, H; *P. aeruginosa*), PCL/Gel50/CMSNs2.5%/ABs (I; *S. aureus*, J; *P.*

*aeruginosa*) and PCL/Gel50/CMSNs5%/ABs (K; *S. aureus*, L; *P. aeruginosa*) compared to biofilm formation on control nanofibrous mats without antibiotics (M; *S. aureus*, N; *P. aeruginosa*). In nanofibers made of gelatin mixed with PCL, there are evidences of nanofibers in the images due to autofluorescence of gelatin.

by these two species plays a critical role in leading wound to chronic stages by shielding bacterial cells from phagocytic activity of neutrophils and causing prolonged inflammation [53].

### Cytotoxicity assays

MTT cell viability and hemolysis assays were applied to evaluate the biocompatibility of the mats. The viability of mouse fibroblasts cells on tissue culture plates covered by mats after 3 and 7 days culture is

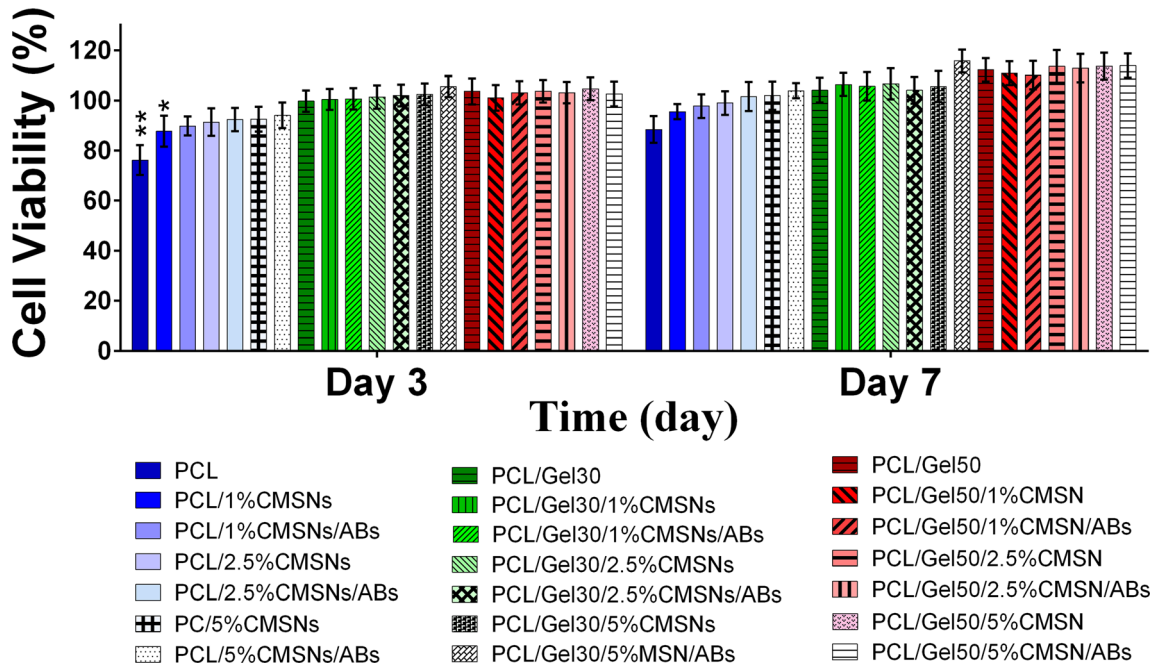
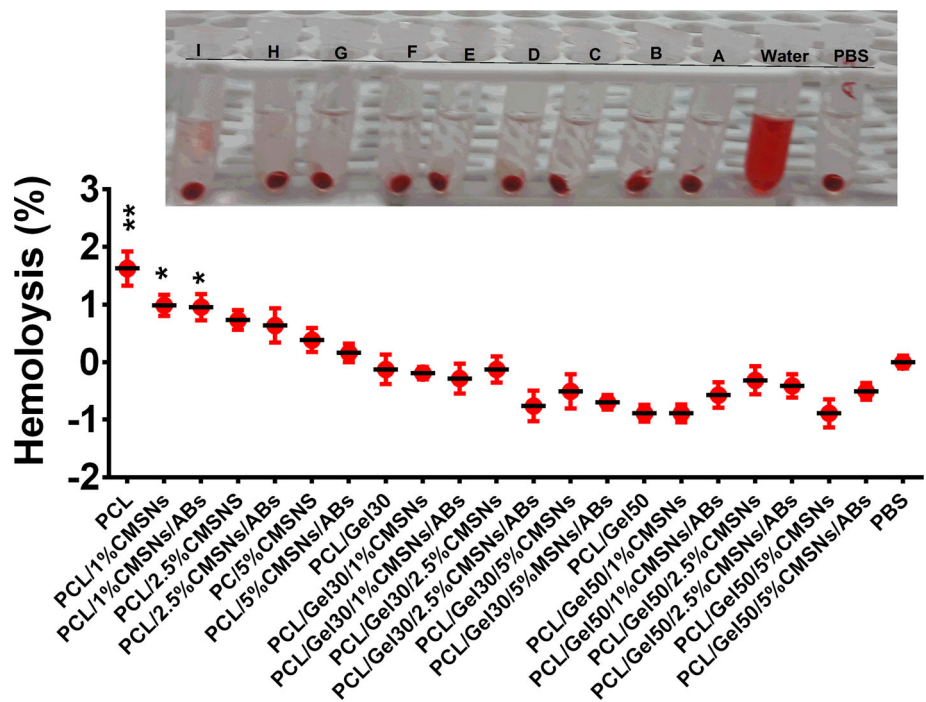


**Figure 8** Viability of L929 mouse fibroblasts cells exposed to different nanofiber mats. Viability of cells in cell media culture was considered as reference. \*( $P < 0.05$ ) and \*\*( $P < 0.01$ ) indicate

significant difference between samples and negative controls (growth media), evaluated by Two-way ANOVA and Turkey’s multiple comparison tests.

**Figure 9** Hemolytic effects of mats on EDTA stabilized human blood cells. Inset image is selected samples include: PBS, Water, a: PCL/Gel30/2.5%CMSNs/ABs, b: PCL/Gel30/5%CMSNs, c: PCL/Gel30/5%CMSNs/ABs, d: PCL/Gel50/2.5%CMSNs/ABs, e: PCL/Gel50/5%CMSNs, f: PCL/Gel50/5% CMSNs/ABs, g: PCL/2.5% CMSNs/ABs, F: PCL/5% CMSNs/, h: PCL/5% CMSNs/ABs. The \*, \*\*present  $p < 0.05$  and  $p < 0.01$ , analyzed by one-way ANOVA as compared to PBS hemolysis rate.



shown in Fig. 8. Compared with control wells containing growth media with no mats, cell viability did not change when they were treated with PCL/Gel30 and PCL/Gel50 and their corresponding mats

containing 1%, 2.5% and 5% CMSNs with and without antibiotics. PCL alone showed a slightly decreased cell viability which was attributed to lower hydrophilicity of PCL [20].

Hemolysis can occur when red blood cells are ruptured as a result of contact with artificial materials and can be followed with accelerated thrombus [54]. Since wound dressings interact with blood especially in extensive burn injuries, their hemocompatibility is a major prerequisite [55]. Thus, the cytotoxicity of nanofibers was further analyzed by hemolysis assay. Results showed no hemolytic effects for all tested mats except a hemolytic effect of less than 2% for PCL nanofibers comparing to control treatments (PBS), which decreased by adding 1%, 2.5% and 5% CMSNs (PBS) (Fig. 9). These results are in line with previous studies which show high biocompatibility of PCL and PCL/Gel nanofibers [24, 56]. The results also demonstrate that strong acidic solvents used to synthesize nanofibers in this study, did not add any cytotoxic effects to nanofibers which is consistent with previous studies [23, 24].

## Conclusions

We developed broad-spectrum antibacterial nanofibrous mats with potential applications as wound dressings with different combinations of PCL, gelatin and CMSNs. Desirable degradability and release of antibiotics were obtained when PCL was mixed with gelatin. Antibacterial activity of nanofibrous mats were improved by adding gelatin, which was attributed to increased degradability of nanofibers. PCL/Gel mats containing 5% antibiotics-loaded CMSNs depicted excellent anti-biofilm activity against both Gram-negative *P. aeruginosa* and Gram-positive *S. aureus*. The results of this study can contribute significantly in developing functional materials against both acute and chronic wounds infections.

## Acknowledgement

The authors thank Markku Saari and Jouko Sandholm of the Cell Imaging Core (CIC) at Turku supported by Biocenter Finland for technical support and advice. We also thank Jussi Meriluoto of faculty of science and engineering in Abo Academy for his advice about HPLC analysis. Supports received from Iran National Science Foundation (INSF) and National Institute of Genetic Engineering and Biotechnology (NIGEB) are also appreciated.

## Compliance with ethical standards

**Conflict of interest** The authors declare no competing financial interest.

**Electronic supplementary material:** The online version of this article (<https://doi.org/10.1007/s10853-020-05253-7>) contains supplementary material, which is available to authorized users.

## References

- [1] Martin JM, Zenilman JM, Lazarus GS (2010) Molecular microbiology: new dimensions for cutaneous biology and wound healing. *J Invest Dermatol* 130:38–48. <https://doi.org/10.1038/jid.2009.221>
- [2] Bowler PG, Duerden BI, Armstrong DG (2001) Wound microbiology and associated approaches to wound management. *Clin Microbiol Rev* 14:244–269. <https://doi.org/10.1128/CMR.14.2.244-269.2001>
- [3] Lipsky BA, Hoey C (2009) Topical antimicrobial therapy for treating chronic wounds. *Clin Infect Dis* 49:1541–1549. <https://doi.org/10.1086/644732>
- [4] Hernandez R (2006) The use of systemic antibiotics in the treatment of chronic wounds. *Dermatol Ther* 19:326–337. <https://doi.org/10.1111/j.1529-8019.2006.00091.x>
- [5] Velkov T, Thompson PE, Nation RL, Li J (2010) Structure-activity relationships of polymyxin antibiotics. *J Med Chem* 53:1898–1916. <https://doi.org/10.1021/jm900999h>
- [6] Hubbard BK, Walsh CT (2003) Vancomycin assembly: nature's way. *Angew Chemie* 42:730–765. <https://doi.org/10.1002/anie.200390202>
- [7] Lenhard JR, Nation RL, Tsuji BT (2016) Synergistic combinations of polymyxins. *Int J Antimicrob Agents* 48:607–613. <https://doi.org/10.1016/j.ijantimicag.2016.09.014>
- [8] Poirel L, Jayol A, Nordmann P (2017) Polymyxins: antibacterial activity, susceptibility testing, and resistance-mechanisms encoded by plasmids or chromosomes. *Clin Microbiol Rev* 30:557–596
- [9] Xie J, Pierce JG, James RC et al (2011) A redesigned vancomycin engineered for dual d-Ala-d-Ala and d-Ala-d-Lac binding exhibits potent antimicrobial activity against vancomycin-resistant bacteria. *J Am Chem Soc* 133:13946–13949. <https://doi.org/10.1021/ja207142h>
- [10] Van Hal SJ, Paterson DL, Lodise TP (2013) Systematic review and meta-analysis of vancomycin-induced nephrotoxicity associated with dosing schedules that maintain troughs between 15 and 20 milligrams per liter. *Antimicrob*

- Agents Chemother 57:734–744. <https://doi.org/10.1128/AA.C.01568-12>
- [11] Vattimo De Fátima Fernandes, Maria Watanabe M, Da Fonseca CD, De Moura Neiva LB et al (2016) Polymyxin B nephrotoxicity: from organ to cell damage. PLoS ONE 11:e0161057. <https://doi.org/10.1371/journal.pone.0161057>
- [12] Memic A, Abudula T, Mohammed HS et al (2019) Latest progress in electrospun nano fibers for wound healing applications. ACS Appl Mater Interfaces 2:952–969. <https://doi.org/10.1021/acsabm.8b00637>
- [13] Liu M, Duan X, Li Y et al (2017) Electrospun nano fibers for wound healing. Mater Sci Eng, C 76:1413–1423. <https://doi.org/10.1016/j.msec.2017.03.034>
- [14] Yang J, Wang K, Yu D et al (2020) Electrospun janus nanofibers loaded with a drug and inorganic nanoparticles as an effective antibacterial wound dressing. Mater Sci Eng C 111:110805. <https://doi.org/10.1016/j.msec.2020.110805>
- [15] García-Salinas S, Gámez E, Asin J et al (2020) Efficiency of antimicrobial electrospun thymol-loaded polycaprolactone mats in vivo. ACS Appl Bio Mater 3:3430–3439. <https://doi.org/10.1021/acsabm.0c00419>
- [16] Homaeigohar S, Boccaccini AR (2020) Antibacterial bio-hybrid nanofibers for wound dressings. Acta Biomater 107:25–49. <https://doi.org/10.1016/j.actbio.2020.02.022>
- [17] Chong LH, Lim MM, Sultana N (2015) Fabrication and evaluation of polycaprolactone/gelatin-based electrospun nanofibers with antibacterial properties. J Nanomater 2015:1–8. <https://doi.org/10.1155/2015/970542>
- [18] Monteiro N, Martins M, Martins A et al (2015) Antibacterial activity of chitosan nanofiber meshes with liposomes immobilized releasing gentamicin. Acta Biomater 18:196–205. <https://doi.org/10.1016/j.actbio.2015.02.018>
- [19] Zhang M, Li Z, Liu L et al (2016) Preparation and characterization of vancomycin-loaded electrospun *Rana chensinensis* skin collagen/poly(L-lactide) nanofibers for drug delivery. J Nanomater 2016:1–8. <https://doi.org/10.1155/2016/9159364>
- [20] Rong D, Chen P, Yang Y et al (2016) Fabrication of gelatin/PCL electrospun fiber mat with bone powder and the study of its biocompatibility. J Funct Biomater. <https://doi.org/10.3390/jfb7010006>
- [21] Suwantong O (2016) Biomedical applications of electrospun polycaprolactone fiber mats. Polym Adv Technol 27:1264–1273. <https://doi.org/10.1002/pat.3876>
- [22] Safaeijavan R, Soleimani M, Divsalar A, Eidi A (2014) Biological behavior study of gelatin coated PCL nanofibrous electrospun scaffolds using fibroblasts. J Paramed Sci 5:67–73. <https://doi.org/10.22037/jps.v5i1.5467>
- [23] Binulal NS, Natarajan A, Menon D et al (2014) PCL-gelatin composite nanofibers electrospun using diluted acetic acid-ethyl acetate solvent system for stem cell-based bone tissue engineering. J Biomater Sci Polym Ed 25:325–340. <https://doi.org/10.1080/09205063.2013.859872>
- [24] Ren K, Wang Y, Sun T et al (2017) Electrospun PCL/gelatin composite nanofiber structures for effective guided bone regeneration membranes. Mater Sci Eng, C 78:324–332. <https://doi.org/10.1016/j.msec.2017.04.084>
- [25] Zhang Y, Ouyang H, Chwee TL et al (2005) Electrospinning of gelatin fibers and gelatin/PCL composite fibrous scaffolds. J Biomed Mater Res-Part B Appl Biomater 72:156–165. <https://doi.org/10.1002/jbm.b.30128>
- [26] Katsogiannis KAG, Vladislavljević GT, Georgiadou S (2015) Porous electrospun polycaprolactone (PCL) fibres by phase separation. Eur Polym J 69:284–295. <https://doi.org/10.1016/j.eurpolymj.2015.01.028>
- [27] Dulnik J, Denis P, Sajkiewicz P et al (2016) Biodegradation of bicomponent PCL/gelatin and PCL/collagen nanofibers electrospun from alternative solvent system. Polym Degrad Stab 130:10–21. <https://doi.org/10.1016/j.polymdegradstab.2016.05.022>
- [28] Yao F, Weiyuan JK (2010) Drug release kinetics and transport mechanisms of non- degradable and degradable polymeric delivery systems. Expert Opin Drug Deliv 7:429–444. <https://doi.org/10.1517/17425241003602259.Drug>
- [29] Venugopal JR, Low S, Choon AT et al (2008) Nanobio-engineered electrospun composite nanofibers and osteoblasts for bone regeneration. Artif Organs 32:388–397. <https://doi.org/10.1111/j.1525-1594.2008.00557.x>
- [30] Kim MS, Kim G (2014) Three-dimensional electrospun polycaprolactone (PCL)/alginate hybrid composite scaffolds. Carbohydr Polym 114:213–221. <https://doi.org/10.1016/j.carbpol.2014.08.008>
- [31] Li H, Wang M, Williams GR et al (2016) Electrospun gelatin nanofibers loaded with vitamins A and E as antibacterial wound dressing materials. RSC Adv 6:50267–50277. <https://doi.org/10.1039/C6RA05092A>
- [32] McCormick MH, Mcguire JM (1955) Vancomycin and method for its preparation. US Patent 3,067,099. <https://patents.google.com/patent/US3067099A/en>
- [33] Drey REA, Foster GE, Stewart GA (1955) The assay of polymyxin and its preparations. J Pharm Pharmacol 7:706–716. <https://doi.org/10.1111/j.2042-7158.1955.tb12084.x>
- [34] Gounani Z, Asadollahi MA, Pedersen JN et al (2019) Mesoporous silica nanoparticles carrying multiple antibiotics provide enhanced synergistic effect and improved biocompatibility. Colloids Surfaces B Biointerfaces 175:498–508. <https://doi.org/10.1016/j.colsurfb.2018.12.035>
- [35] Mehrasa M, Asadollahi MA, Nasri-Nasrabadi B et al (2016) Incorporation of mesoporous silica nanoparticles into



- random electrospun PLGA and PLGA/gelatin nanofibrous scaffolds enhances mechanical and cell proliferation properties. *Mater Sci Eng, C* 66:25–32. <https://doi.org/10.1016/j.msec.2016.04.031>
- [36] Dong R-H, Jia Y-X, Qin C-C et al (2016) In situ deposition of a personalized nanofibrous dressing via a handy electrospinning device for skin wound care. *Nanoscale* 8:3482–3488. <https://doi.org/10.1039/C5NR08367B>
- [37] Gounani Z, Asadollahi MA, Meyer RL, Arpanaei A (2018) Loading of polymyxin B onto anionic mesoporous silica nanoparticles retains antibacterial activity and enhances biocompatibility. *Int J Pharm* 537:148–161. <https://doi.org/10.1016/j.ijpharm.2017.12.039>
- [38] Song B, Wu C, Chang J (2012) Dual drug release from electrospun poly(lactic-co-glycolic acid)/mesoporous silica nanoparticles composite mats with distinct release profiles. *Acta Biomater* 8:1901–1907. <https://doi.org/10.1016/j.actbio.2012.01.020>
- [39] Song BJ, Chen M, Regina VR et al (2012) Safe and effective Ag nanoparticles immobilized antimicrobial nanononwovens. *Adv Eng Mater* 14:12–14. <https://doi.org/10.1002/adem.201180085>
- [40] Mehra M, Asadollahi MA, Ghaedi K et al (2015) Electrospun aligned PLGA and PLGA/gelatin nanofibers embedded with silica nanoparticles for tissue engineering. *Int J Biol Macromol* 79:687–695. <https://doi.org/10.1016/j.ijbiomac.2015.05.050>
- [41] Li K, Sun H, Sui H et al (2015) Composite mesoporous silica nanoparticle/chitosan nanofibers for bone tissue engineering. *RSC Adv* 5:17541–17549. <https://doi.org/10.1039/b000000x>
- [42] Munj HR, Lannutti JJ, Tomasko DL (2017) Understanding drug release from PCL/gelatin electrospun blends. *J Biomater Appl* 31:933–949. <https://doi.org/10.1177/0885328216673555>
- [43] Ganesh N, Jayakumar R, Koyakutty M et al (2012) Embedded silica nanoparticles in poly(caprolactone) nanofibrous scaffolds enhanced osteogenic potential for bone tissue engineering. *Tissue Eng Part A* 18:1867–1881. <https://doi.org/10.1089/ten.TEA.2012.0167>
- [44] Liu Y, Liu G, Li M, He C (2017) Synthesis, characterization, and hydrolytic degradation of polylactide/poly( $\epsilon$ -caprolactone)/nano-silica composites. *J Macromol Sci Part A Pure Appl Chem* 54:813–818. <https://doi.org/10.1080/10601325.2017.1336726>
- [45] Charemsriwilaiwat N, Opanasopit P, Rojanarata T, Ngawhirunpat T (2012) Lysozyme-loaded, electrospun chitosan-based nanofiber mats for wound healing. *Int J Pharm* 427:379–384. <https://doi.org/10.1016/j.ijpharm.2012.02.010>
- [46] Kontogiannopoulos KN, Assimopoulou AN, Tsvintzelis I et al (2011) Electrospun fiber mats containing shikonin and derivatives with potential biomedical applications. *Int J Pharm* 409:216–228. <https://doi.org/10.1016/j.ijpharm.2011.02.004>
- [47] Jalvandi J, White M, Truong YB et al (2015) Release and antimicrobial activity of levofloxacin from composite mats of poly( $\epsilon$ -caprolactone) and mesoporous silica nanoparticles fabricated by core-shell electrospinning. *J Mater Sci* 50:7967–7974. <https://doi.org/10.1007/s10853-015-9361-x>
- [48] Li D, Nie W, Chen L et al (2017) Fabrication of curcumin-loaded mesoporous silica incorporated polyvinyl pyrrolidone nanofibers for rapid hemostasis and antibacterial treatment. *RSC Adv* 7:7973–7982. <https://doi.org/10.1039/C6RA27319J>
- [49] Van Vlierberghe S, Graulus G-J, Samal SK et al (2014) Porous hydrogel biomedical foam scaffolds for tissue repair. In: Netti PA (ed) *Biomedical foams for tissue engineering applications*, 1st edn. Woodhead Publishing, Cambridge, pp 335–390
- [50] Percival SL, Hill KE, Williams DW et al (2012) A review of the scientific evidence for biofilms in wounds. *Wound Repair Regen* 20:647–657. <https://doi.org/10.1111/j.1524-475X.2012.00836.x>
- [51] Heunis TDJ, Smith C, Dicks LMT (2013) Evaluation of a nisin-eluting nanofiber scaffold to treat *Staphylococcus aureus*-induced skin infections in mice. *Antimicrob Agents Chemother* 57:3928–3935. <https://doi.org/10.1128/AAC.00622-13>
- [52] Ahire JJ, Hattingh M, Neveling DP, Dicks LMT (2016) Copper-containing anti-biofilm nanofiber scaffolds as a wound dressing material. *PLoS ONE* 11:1–12. <https://doi.org/10.1371/journal.pone.0152755>
- [53] Guo S, DiPietro LA (2010) Critical review in oral biology & medicine: factors affecting wound healing. *J Dent Res* 89:219–229. <https://doi.org/10.1177/0022034509359125>
- [54] Poornima B, Korrapati PS (2017) Fabrication of chitosan-polycaprolactone composite nanofibrous scaffold for simultaneous delivery of ferulic acid and resveratrol. *Carbohydr Polym* 157:1741–1749. <https://doi.org/10.1016/j.carbpol.2016.11.056>
- [55] Denzinger M, Held M, Schef H et al (2019) Hemocompatibility of different burn wound dressings. *Wound Repair Regen* 27:470–476. <https://doi.org/10.1111/wrr.12739>
- [56] Kmiec EB, Borjigin M, Strouse B et al (2012) Proliferation of genetically modified human cells on electrospun nanofiber scaffolds. *Mol Ther Nucleic Acids* 1:e59. <https://doi.org/10.1038/mtna.2012.51>

**Publisher's Note** Springer Nature remains neutral with regard to jurisdictional claims in published maps and institutional affiliations.